CoRoT/ESTA - Model Comparison - Task 1

Internal structure and seismic properties

Monteiro M.J.P.F.G. (Porto), Castro M. (Toulouse),
Christensen-Dalsgaard J. (Aarhus), Cunha M.S. (Porto),
Degl'Innocenti S. (Pisa), Eggenberger P. (Geneva), Lebreton Y. (Paris),
Marconi M. (Napoli), Marques J.P. (Porto & Coimbra),
Miglio A. (Liège), Montalbán J. (Liège), Morel P. (Nice),
Moya A. (Paris), Prada Moroni P.G. (Pisa),
Roxburgh I.W. (London & Paris), Scuflaire R. (Liège),
Teixeira T.C. (Porto & London)

Abstract

In this work we present the results on the internal structure and seismic properties for Task 1 of the *Evolution and Seismic Tools Activity* (ESTA) of the CoRoT *Seismology Working Group*. For this task several target stars have been defined. Models produced with different codes have been calculated to represent the target stars. The results on the comparison of the internal structure and seismic properties are shown.

A list of the Codes being used to calculate the models are presented. The physics adopted in the calculation of the models is described in Poster 1 (Monteiro et al., 2005). Here we restrict the comparison to the set of models where the global parameters are similar within 1% in order to illustrate where the internal structure and seismic properties differ between different codes. The goal is to identify the aspects of the physics and numerical implemention that can be the source of discrepancies. A characterisation of the differences in the seismic properties is also provided to illustrate the impact of the model differences on the seismic interpretation.

1 Evolution Codes and target models

The Evolution codes used in this comparison are listed here with the references where the description of each code can be found. The models discussed and compared in the next sections have been calculated by the following codes:

- **ASTEC - Aarhus Stellar Evolution Code** [*Christensen-Dalsgaard*] - a general description of the code available in print is Christensen-Dalsgaard (1982). Further up-to-date details can also be found in Christensen-Dalsgaard (2005a).

- **CESAM - Code d'Évolution Stellaire Adaptatif et Modulaire** [*Lebreton & Morel*] - a published general description in english of the code available in print is Morel (1997). A detailed description (in french) is available under request at the WEB sites:
  `http://www.obs-nice.fr/morel/CESAM`
  `http://www.obs-nice.fr/cesam/`
  An up-to-date description can also be found at Pichon & Morel (2005).

- **CLES - Code Liègeois d'Evolution Stellaire** [*Montalbán, Scuflaire & BAG*] - CLES is still in an active phase of development at the Institute of Astrophysics of Liège. Further up-to-date details can be found in Scuflaire (2005).
- **FRANEC - Pisa Evolution Code** [*Degl'Innocenti, Marconi & Prada Moroni*] - The main properties and physical assumptions of the FRANEC code are discussed in Cariulo et al. (2004) (see also Ciacio et al. 1997). Further up-to-date details can also be found in Degl'Innocenti & Marconi (2005).
- **STAROX - Roxburgh's Evolution Code** [*Roxburgh*] - A description of the main properties and physical assumptions of the code can be found in Roxburgh (2005).

Seven targets have been defined (see Poster 1 - Monteiro et al. 2005) covering a relevant range of stellar masses and ages. The parameters for the evolution that have been specified for each case are listed in Table 1. One case has also been considered for the presence of overshoot. The specification for the Helium core adopts the following definition: $M_{\rm HeC}$ is the mass of the central region of the star where the Hydrogen abundance is $X \leq 0.01$.

Also indicated in the Table is the type of models that have been selected:

- **PreMS** - pre-main sequence models,
- **ZAMS** - near the beginning of the main sequence,
- **MS** - main sequence models,
- **TAMS** - near the end of the main sequence,
- **PostMS** - post-main sequence models.

2 Comparison: internal structure

We consider here the comparison of two functions of the internal structure aiming at providing an indication on where significant discrepancies may be and the reason for their presence. As two representative functions we have selected the sound speed c^2 (shown in Figs 1 and 2) and the abundance of Hydrogen X (shown in Figs 3 and 4). The model from the code CESAM is used as the reference for cases 1.1-1.2 and 1.4-1.7, while the model from ASTEC is used as the reference for case 1.3.

Here we only use models whose global parameters (see Monteiro et al. 2005) are very similar in order to secure that the model differences are mainly determined by how each code calculates the evolution and the structure of the target model.

As a summary of the figures we provide in Table 2 the spread of the model differences for $0 \leq r/R \leq 0.95$. We restrict the comparison to the interior in order to remove from the present comparison the unresolved differences found near the surface. Further work is required to understand what is the source of the differences between models for the surface layers.

3 Comparison: seismic properties

For the comparison of the global seismic properties of the models we have used one seismic code (POSC) in order to calculate the frequencies of oscillations of all models for Cases 1.1 and 1.2. The modes being used in this comparison have mode degree l=0, 1, 2, 3 and mode order n=5 − 20.

In Figs 5 the frequency differences are shown for modes of different degrees. After removing the scaling due to different stellar radius, the differences of the frequencies are dominated, as expected, by the near surface differences of the models. The component due to differences in the deep interior, as given by the differences between curves for different mode degrees, is very small.

We also consider here the frequency separations as defined by:

- $\Delta_0 \equiv \nu_{n+1,0} - \nu_{n,0}$ → large frequency separation between the frequencies ($\nu_{n,l}$) for modes of degree l=0 and consecutive mode order n.
- $\delta_{02} \equiv \nu_{n,0} - \nu_{n-1,2}$ → small frequency separation between the frequencies ($\nu_{n,l}$) for modes of degree l=0 and l=2 with mode orders n and $n-1$, respectively.

The large frequency separations are shown in Fig. 6 while the small frequency separations are shown in Fig. 7 for the two main sequence models considered here. Given the similarity for the global parameters of the models the calculated separations are very similar. To illustrate the effect on the separations due to differences in the radius of the models, the scaled large frequency differences is also shown in Fig. 6.

The frequencies for the evolved models are not discussed here as such an analysis requires the validation of the seismic calculation of the frequencies for these models. Part of this validation is already being developed under Task 2 of ESTA (see Moya et al. 2005)

4 Discussion

It is shown here that the models calculated by four different codes are - to first order - consistent, as one would expect. The maximum of the relative differences in the internal structure, listed in Tables 2, is small. This difference has been strongly reduced comparing only the output of codes where the physics have been adapted to the required specifications.

In the seismic parameters the differences for the frequencies are dominated by the differences in the stellar radius and the surface differences between models. This was to be expected as different codes still use slightly different physics which affect more strongly the near surface layers. More work to understand how to model the surface layers is required (see also Lebreton & Monteiro 2005; Christensen-Dalsgaard 2005b).

References

Cariulo, P., Degl'Innocenti, S., Castellani, V., 2004, A&A, **421**, 1121

Christensen-Dalsgaard, J., 1982, MNRAS **199**, 735

Christensen-Dalsgaard, J., 2005a, *ASTEC: Aarhus Stellar Evolution Code*, in CoRoT/ESTA Meeting 4, Aarhus - Denmark, 24-28 October 2005,
at `http://www.astro.up.pt/corot/welcome/meetings/m4/`

Christensen-Dalsgaard, J., 2005b, *Summary of Aarhus workshop: Some selected results*, in CoRoT/ESTA Meeting 4, Aarhus - Denmark, 24-28 October 2005,
at `http://www.astro.up.pt/corot/welcome/meetings/m4/`

Ciacio, F., degl'Innocenti, S. & Ricci, B., 1997, A&AS, **123**, 449

Degl'Innocenti, S., Marconi, M., 2005, *FRANEC Code* in CoRoT/ESTA Meeting 3, Nice - France, 26-27 September 2005,
at `http://www.astro.up.pt/corot/welcome/meetings/m3/`

Lebreton, Y., Monteiro, M. J. P. F. G., 2005, *Task 1 results and implications: What needs to be done and how?*, in CoRoT/ESTA Meeting 3, Nice - France, 26-27 September 2005,
at `http://www.astro.up.pt/corot/welcome/meetings/m3/`

Monteiro, M. J. P. F. G., Castro, M., Christensen-Dalsgaard J., Cunha M. S., Degl'Innocenti, S., Eggenberger, P., Lebreton, Y., Marconi, M., Marques, J. P., Miglio, A., Montalbán, J., Morel, P., Prada Moroni, P. G., Roxburgh, I. W., Scuflaire, R., Teixeira, T. C., 2005b, *CoRoT/ESTA - Model Comparison - Task 1: Global parameters and evolutionary sequences*, this proceedings.

Morel P., 1997, A&A, **124**, 597

Moya, A., Christensen-Dalsgaard, J., Lebreton, Y., Monteiro, M.J.P.F.G., Provost, J., Roxburgh, I.W., Scuflaire, R., Suarez, J.-C., 2005, *ESTA Task 2 - Step 1: First results on frequency comparison*, this proceedings.

Pichon, B., Morel, M., 2005, *CESAM 2κ in brief*, in CoRoT/ESTA Meeting 3, Nice - France, 26-27 September 2005,
at `http://www.astro.up.pt/corot/welcome/meetings/m3/`

Roxburgh, I. W., 2005, *STAROX-NACRE17: Stellar Evolution Code*, in CoRoT/ESTA Meeting 4, Aarhus - Denmark, 24-28 October 2005,
at `http://www.astro.up.pt/corot/welcome/meetings/m4/`

Scuflaire, R., 2005, *CLÉS: Code Liégeois d'Evolution Stellaire*, in CoRoT/ESTA Meeting 4, Aarhus - Denmark, 24-28 October 2005,
at `http://www.astro.up.pt/corot/welcome/meetings/m4/`

Table 1: Description of the target models proposed under Task1 of the CoRoT/ESTA Model Comparison project. The standard symbols are used. The stellar mass (M) and the He core mass ($M_{\rm HeC}$) are in units of the solar mass ($M_\odot$), while the overshoot extent ($\ell_{\rm ov}$) is in pressure scale heights (H_p). The temperature is in K. For an indication on where these targets are located in the HR diagram please see the other poster (**?**).

Cases:	**1.1**	**1.2**	**1.3**	**1.4**	**1.5**	**1.6**	**1.7**
Parameters:							
$\boldsymbol{M/M_\odot}$	0.9	1.2	1.2	2.0	2.0	3.0	5.0
$\boldsymbol{X_0}$	0.70	0.70	0.73	0.70	0.72	0.71	0.70
$\boldsymbol{Y_0}$	0.28	0.28	0.26	0.28	0.26	0.28	0.28
$\boldsymbol{Z_0}$	0.02	0.02	0.01	0.02	0.02	0.01	0.02
$\boldsymbol{\ell_{\rm ov}/H_p}$	0.0	0.0	0.0	0.0	0.15	0.0	0.0
Target models:							
$\boldsymbol{X_c}$	0.35	0.69	-	-	0.01	0.69	0.35
$\boldsymbol{T_c}$	-	-	-	1.9×10^7	-	-	-
$\boldsymbol{M_{\rm HeC}/M_\odot}$	-	-	0.1	-	-	-	-
Type:	MS	ZAMS	PostMS	PreMS	TAMS	ZAMS	MS

Table 2: Upper limits for the model differences in sound speed squared (c^2) and in hydrogen abundance (X) for the interior structure ($0 \leq m/M \leq 0.95$) of the models being compared. These values are a summary of what the interior differences shown in figs 1-2 and Figs 3-4. The asterisc indicates the models used in the determination of the upper limit for the differences.

Case:	**1.1**	**1.2**	**1.3**	**1.4**	**1.5**	**1.6**	**1.7**
Differences:							
$\max\left(\frac{\delta c^2}{c^2}\right)$	0.0025	0.0026	0.0063	0.004	0.06	0.0078	0.018
$\max(\delta X)$	0.0015	0.0011	0.011	0.00034	0.08	0.0075	0.019
Codes:							
ASTEC	$\star$	$\star$	$\star$	—	$\star$	$\star$	$\star$
CESAM	$\star$	$\star$	—	$\star$	$\star$	$\star$	$\star$
CLES	$\star$	$\star$	$\star$	$\star$	$\star$	$\star$	$\star$
FRANEC	$\star$	—	—	$\star$	—	$\star$	$\star$
STAROX	$\star$	$\star$	—	$\star$	$\star$	$\star$	$\star$

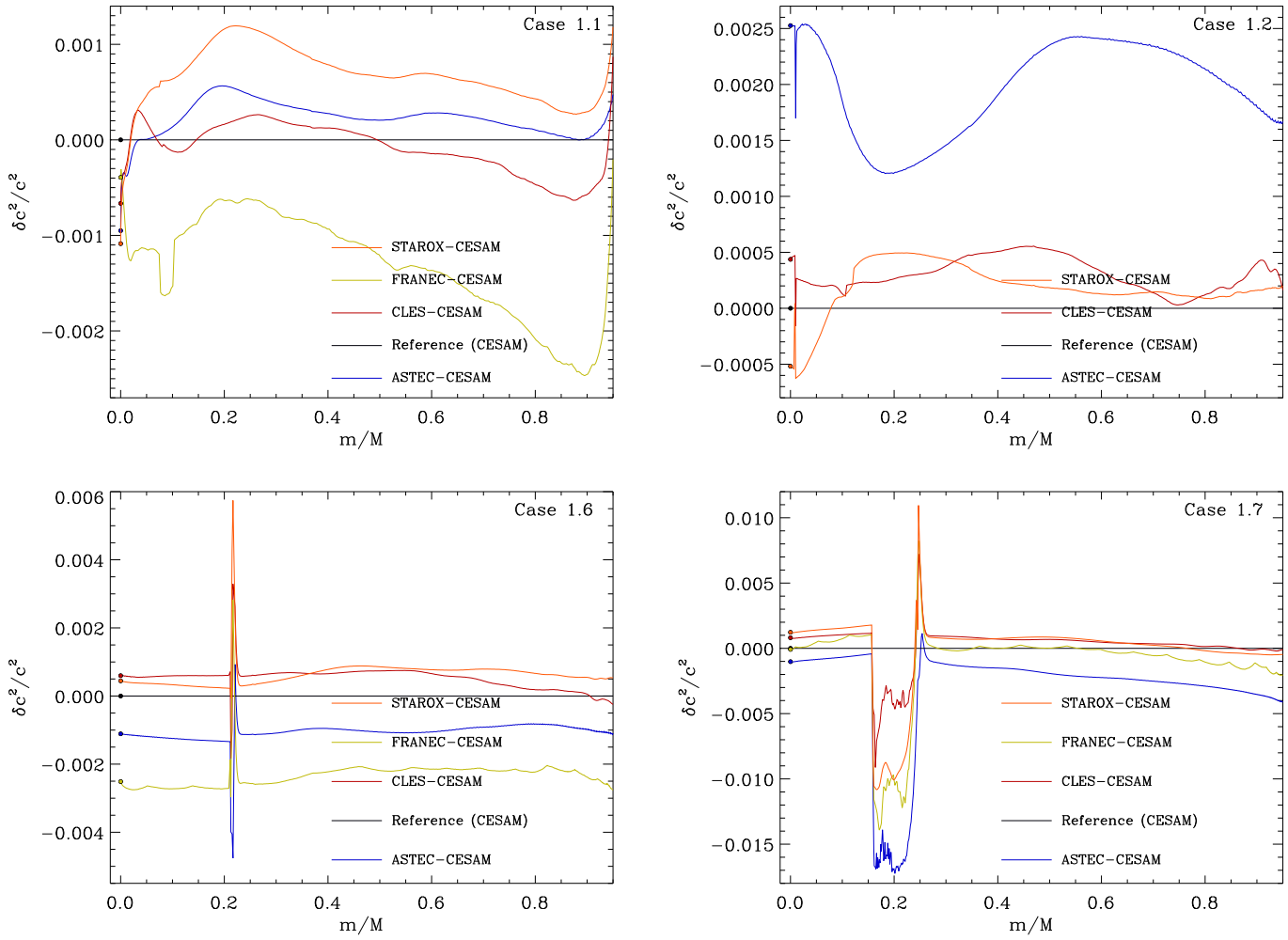

Figure 1: Plot of the relative sound speed differences (at fixed relative mass) between pairs of models in the main sequence (see Table 1). The panels are for Cases 1.1, 1.2, 1.6 and 1.7, as indicated.

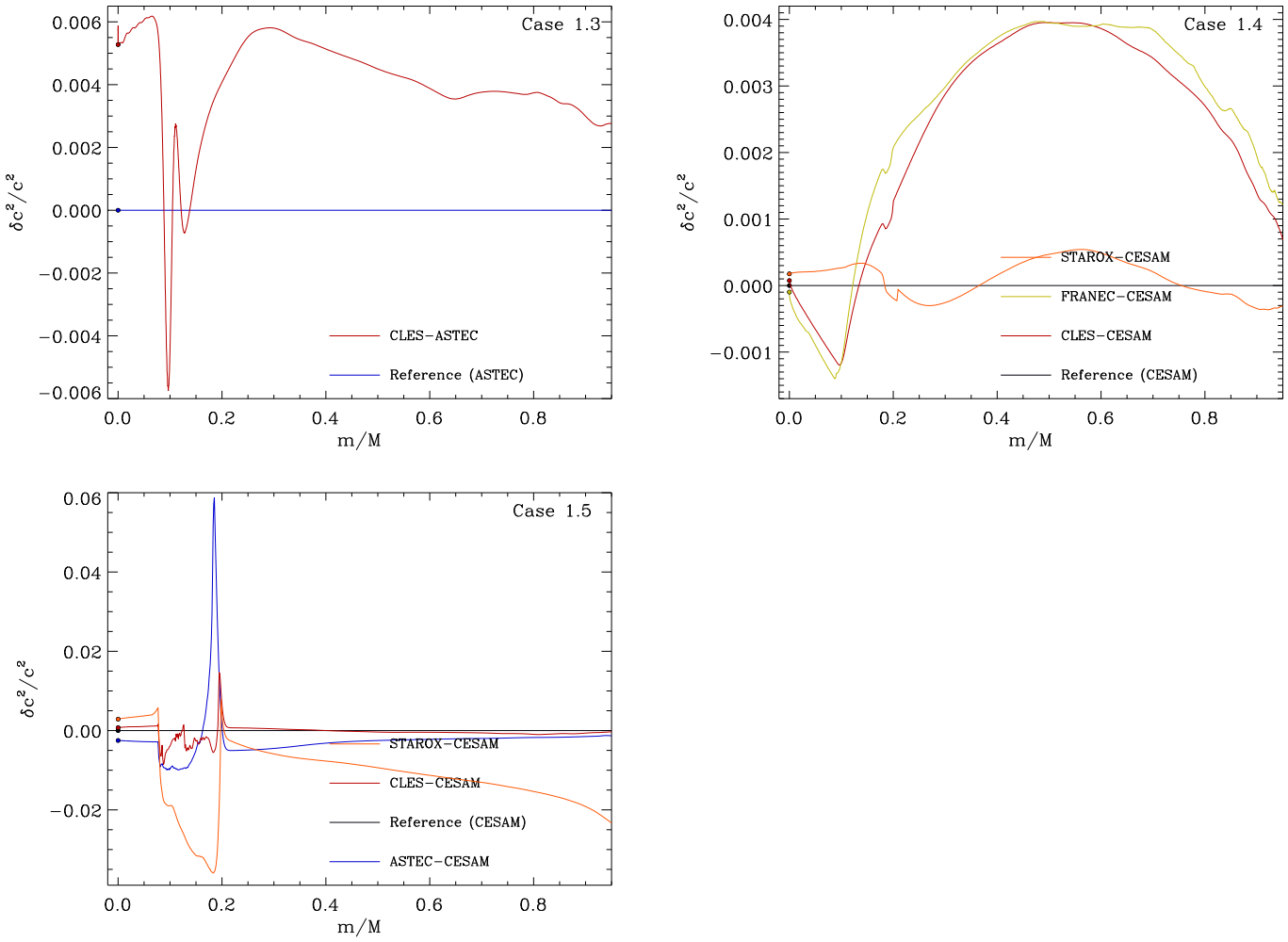

Figure 2: Plot of the relative sound speed differences (at fixed relative mass) between pairs of models off the main sequence (see Table 1). The panels are for Cases 1.3, 1.4 and 1.5 as indicated.

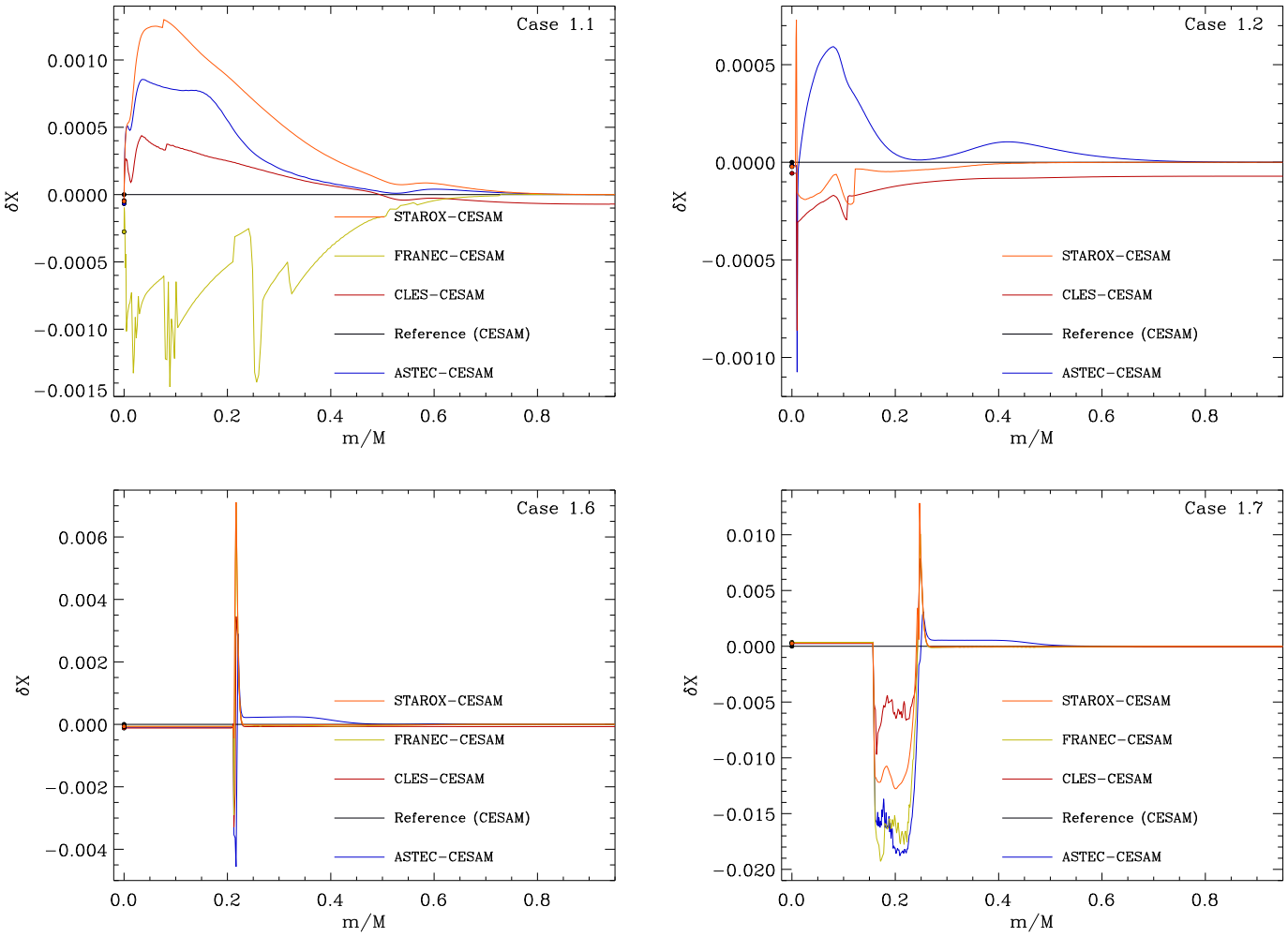

Figure 3: Plot of the Hydrogen abundance differences (at fixed relative mass) between pairs of models in the main sequence (see Table 1). The panels are for Cases 1.1, 1.2, 1.6 and 1.7, as indicated.

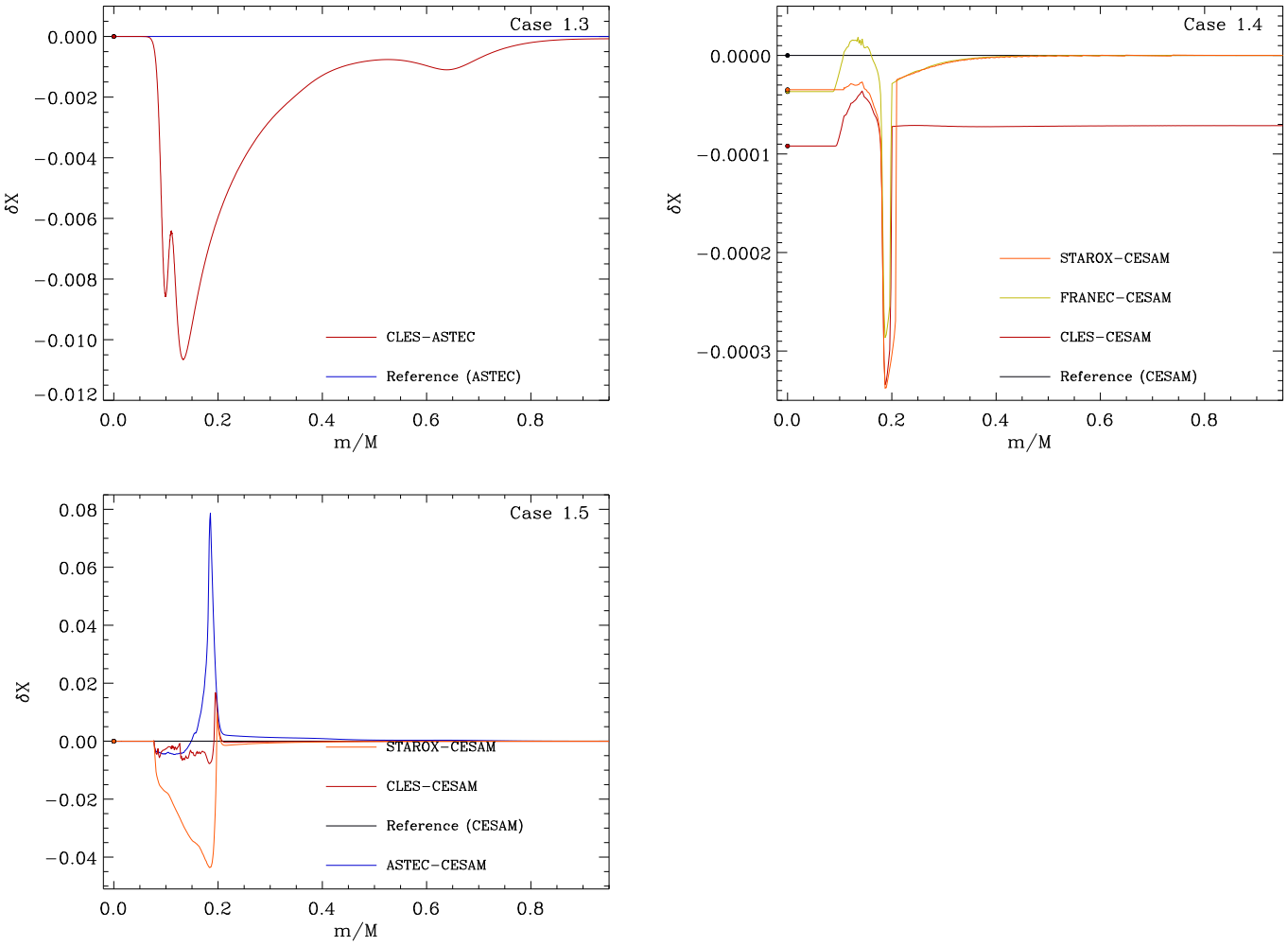

Figure 4: Plot of the Hydrogen abundance differences (at fixed relative mass) between pairs of models off the main sequence (see Table 1). The panels are for Cases 1.3, 1.4 and 1.5 as indicated.

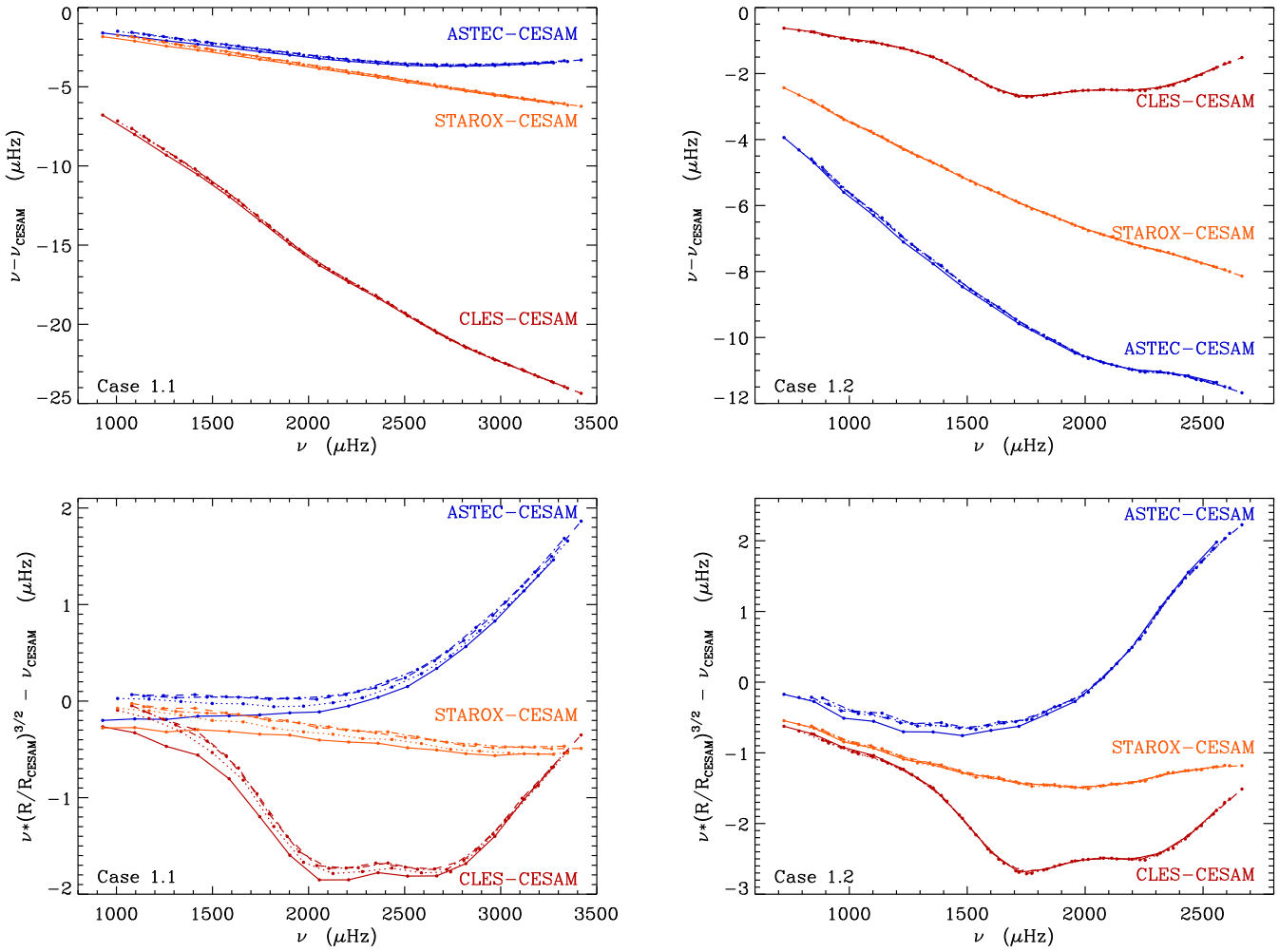

Figure 5: Plot of the frequency differences, between models produced by different codes, for Cases 1.1 and 1.2 as indicated. The full line is for l=0, dotted line for l=1, dashed line for l=2 and dot-dashed line for l=3. Also shown are the frequency differences when the scaling due to the stellar radius (R) is removed. The remaining differences in the frequencies are mainly due to near surface effects.

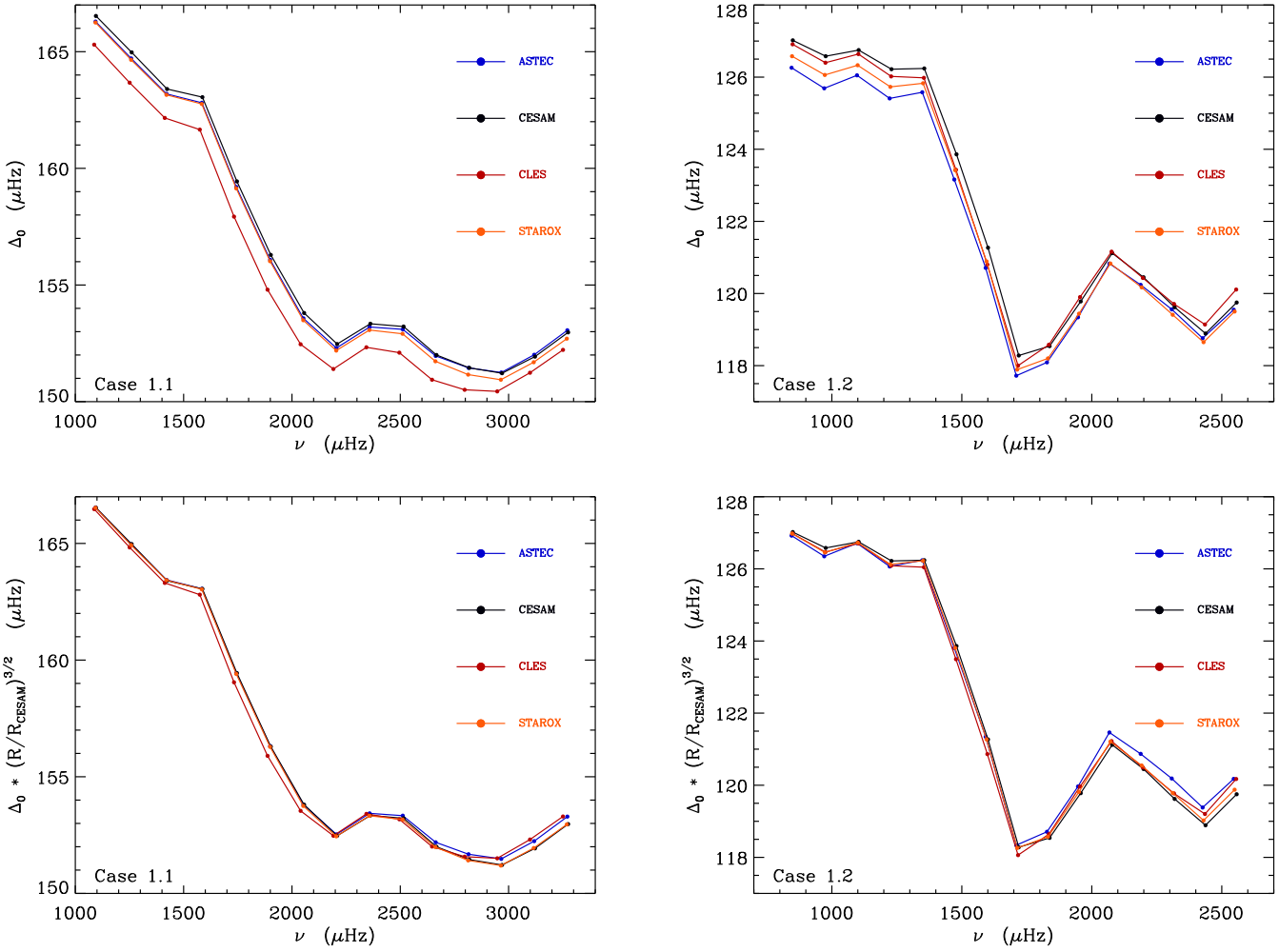

Figure 6: Plot of the large (Δ_0) frequency separation for Cases 1.1 and 1.2 as indicated. Also shown are the same values but after removing the dominant contribution from the differences in the radius of the models.

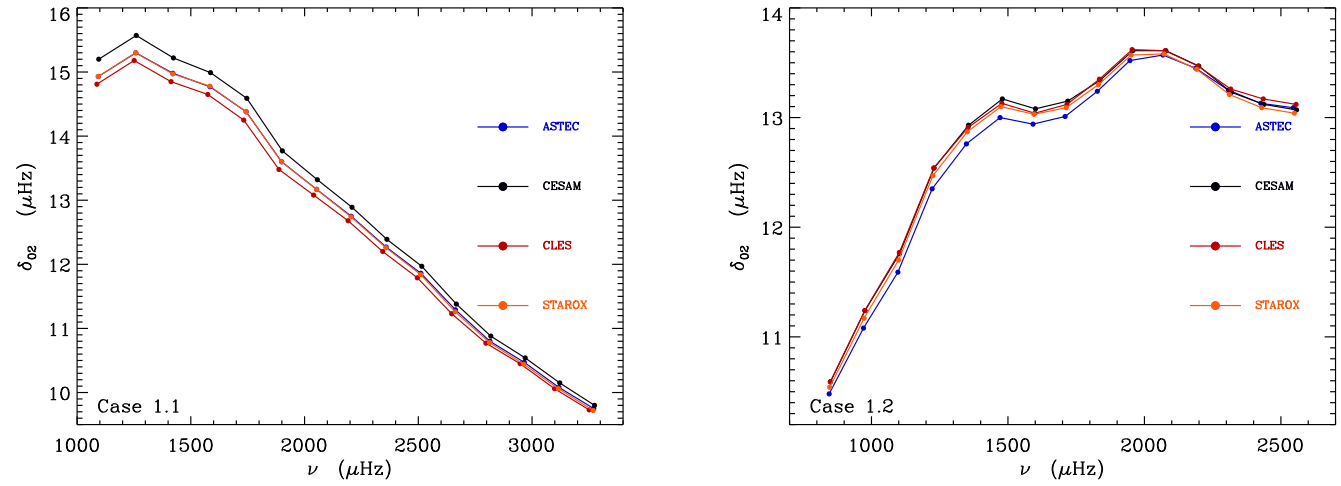

Figure 7: Plot of the small (δ_{02}) frequency separations (see the text) for Cases 1.1 and 1.2 as indicated. Again the major difference is due to the differences in stellar radius.